iScience, Volume *26*

Supplemental information

Frankenbacteriosis targeting interactions between pathogen and symbiont to control infection in the tick vector

Lorena Mazuecos, Pilar Alberdi, Angélica Hernández-Jarguín, Marinela Contreras, Margarita Villar, Alejandro Cabezas-Cruz, Ladislav Šimo, Almudena González-García, Sandra Díaz-Sánchez, Girish Neelakanta, Sarah I. Bonnet, Erol Fikrig, and José de la Fuente

Supplemental information

Frankenbacteriosis targeting interactions between pathogen and symbiont to control infection in the tick vector

Lorena Mazuecos, Pilar Alberdi, Angélica Hernández-Jarguín, Marinela Contreras, Margarita Villar, Alejandro Cabezas-Cruz, Ladislav Simo, Almudena González-García[1], Sandra Díaz-Sánchez, Girish Neelakanta, Sarah I. Bonnet, Erol Fikrig, José de la Fuente

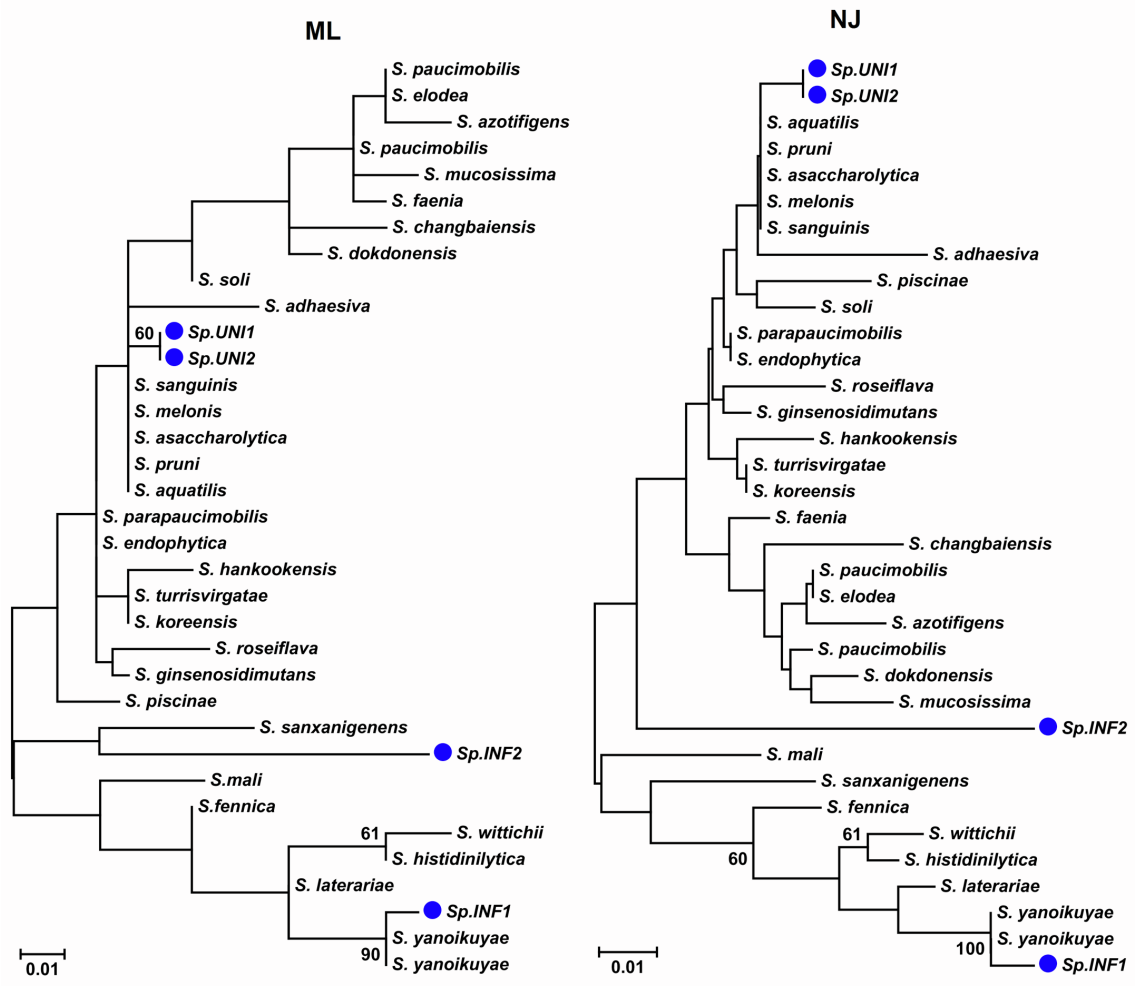

Figure S1. Phylogenetic analysis of *Sphingomonas* spp. identified in tick midgut, Related to STAR Methods. Maximum likelihood (ML) and neighbor joining (NJ) phylogenetic trees were inferred using *16S rDNA* nucleotide sequences of the *Sphingomonas* reported in this study (blue circles) and other bacteria of the genus *Sphingomonas*. *16S rDNA* nucleotide sequences were collected in Genbank to represent different species of the genus *Sphingomonas* as follow: *S. piscinae* (NR_153738), *S. sanguinis* (D84529), *S. paucimobilis* (D84528), *S. paucimobilis* (HF558376), *S. parapaucimobilis* (D84525), *S. roseiflava* (D84520), *S. melonis* (AB055863), S. asaccharolytica (Y09639), *S. pruni* (Y09637), *S. turrisvirgatae* (MG077083), *S. koreensis* (AB681055), *S. soli* (AB166883), *S. ginsenosidimutans* (HM204925), *S. hankookensis* (NR_116570), *S. dokdonensis* (DQ178975), *S. mucosissima* (AM229669), *S. adhaesiva* (D84527), *S. endophytica* (HM629444), *S. faenia* (AJ429239), *S. sanxanigenens* (DQ789172), *S. changbaiensis* (EU682685), *S. azotifigens* (AB217471), *S. elodea* (AF503278), *S. mali* (MF062665), *S. wittichii* (AB021492), *S. histidinilytica* (EF530202), *S. laterariae* (HM159118), *S. fennica* (AJ009706), *S. yanoikuyae* (U37525), *S. yanoikuyae* (U37524). Sequences were aligned with MAFFT (v7) configured for the highest accuracy using the scoring matrix 200PAM/kD2, alignment strategy MAFFT-FFT-NS-I, gap opening penalty 1.53 and offset value 0.123. Non-aligned regions were removed using Molecular Evolutionary Genetics Analysis (MEGA) version 6 software (Tamura et al., 2013; [53]). The best-fit model of sequence evolution was selected based on Corrected Akaike Information Criterion (cAIC) and Bayesian Information Criterion (BIC) implemented in MEGA. A total of 139 positions were included in the final dataset. ML and NJ methods, implemented in MEGA, were used to obtain the best tree topologies. Reliability of internal branches was assessed using the bootstrapping method with 1000 bootstrap replicates (Felsenstein, 1985; [54]). Only bootstrap values ≥ 60 are shown.

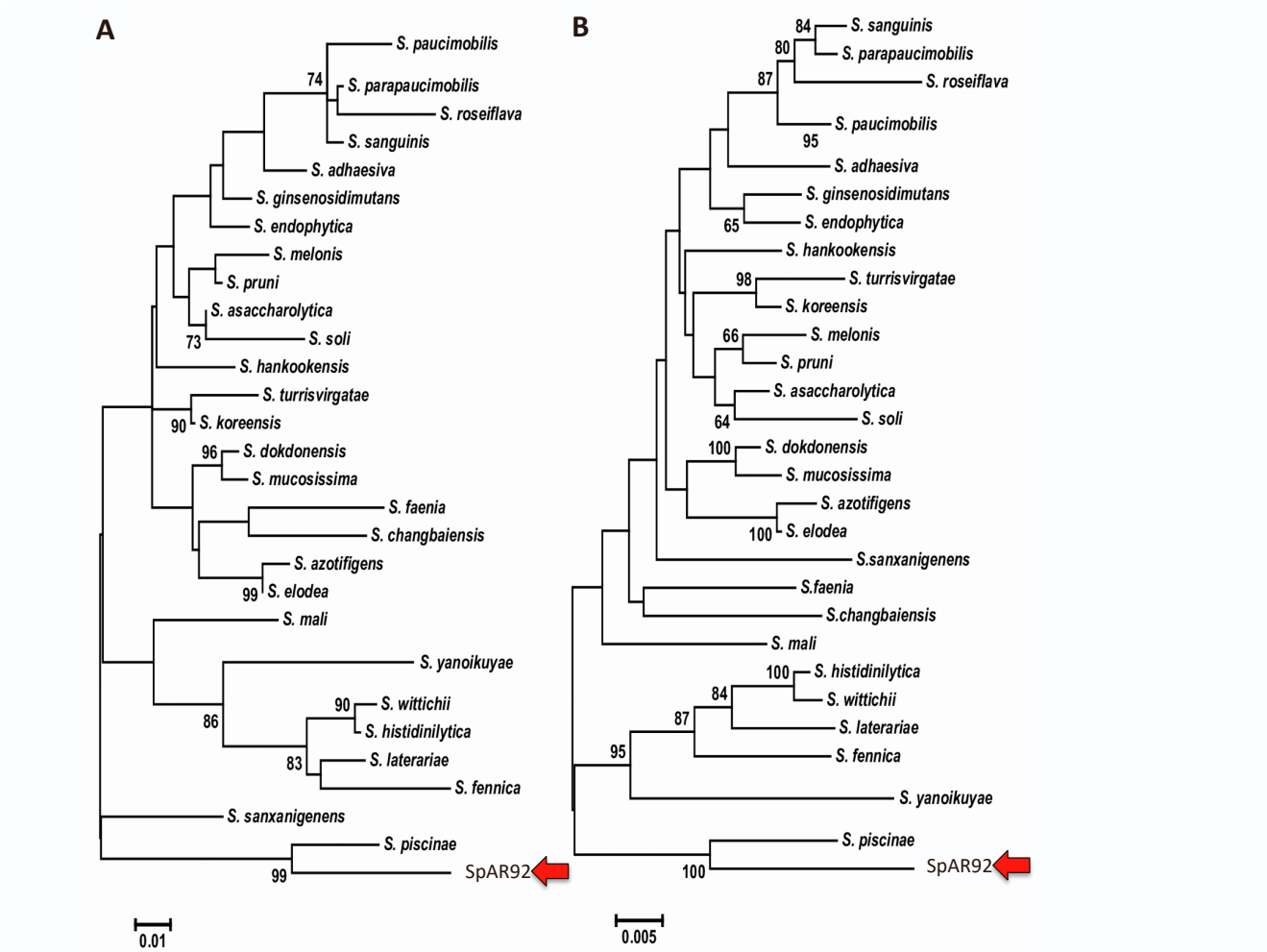

Figure S2. Phylogenetic analysis of the *Sphingomonas* sp. used as a model, Related to STAR Methods. (A) Maximum likelihood (ML) and (B) neighbor joining (NJ) phylogenetic trees were inferred using *16S rDNA* nucleotide sequences of the *Sphingomonas* SpAR92 used as a model in this study for experimental analysis (arrow) and other bacteria of the genus *Sphingomonas*. The *16S rDNA* nucleotide sequences were collected from Genbank to represent different species of the genus *Sphingomonas* as follow: *S. piscinae* (NR_153738), *S. sanguinis* (D84529), *S. paucimobilis* (D84528), *S. paucimobilis* (HF558376), *S. parapaucimobilis* (D84525), *S. roseiflava* (D84520), *S. melonis* (AB055863), S. asaccharolytica (Y09639), *S. pruni* (Y09637), *S. turrisvirgatae* (MG077083), *S. koreensis* (AB681055), *S. soli* (AB166883), *S. ginsenosidimutans* (HM204925), *S. hankookensis* (NR_116570), *S. dokdonensis* (DQ178975), *S. mucosissima* (AM229669), *S. adhaesiva* (D84527), *S. endophytica* (HM629444), *S. faenia* (AJ429239), *S. sanxanigenens* (DQ789172), *S. changbaiensis* (EU682685), *S. azotifigens* (AB217471), *S. elodea* (AF503278), *S. mali* (MF062665), *S. wittichii* (AB021492), *S. histidinilytica* (EF530202), *S. laterariae* (HM159118), *S. fennica* (AJ009706), *S. yanoikuyae* (U37525), *S. yanoikuyae* (U37524). Sequences were aligned with MAFFT (v7) configured for the highest accuracy using the scoring matrix 200PAM/kD2, alignment strategy MAFFT-FFT-NS-I, gap-opening penalty 1.53 and offset value 0.123. Non-aligned regions were removed using Molecular Evolutionary Genetics Analysis (MEGA) version 6 software (Tamura et al., 2013; [53]). The best-fit model of sequence evolution was selected based on Corrected Akaike Information Criterion (cAIC) and Bayesian Information Criterion (BIC) implemented in MEGA. ML and NJ methods, implemented in MEGA, were used to obtain the best tree topologies. There were a total of 1070 positions in the final dataset. Reliability of internal branches was assessed using the bootstrapping method with 1000 bootstrap replicates (Felsenstein, 1985; [54]). Only bootstrap values ≥ 60 are shown.

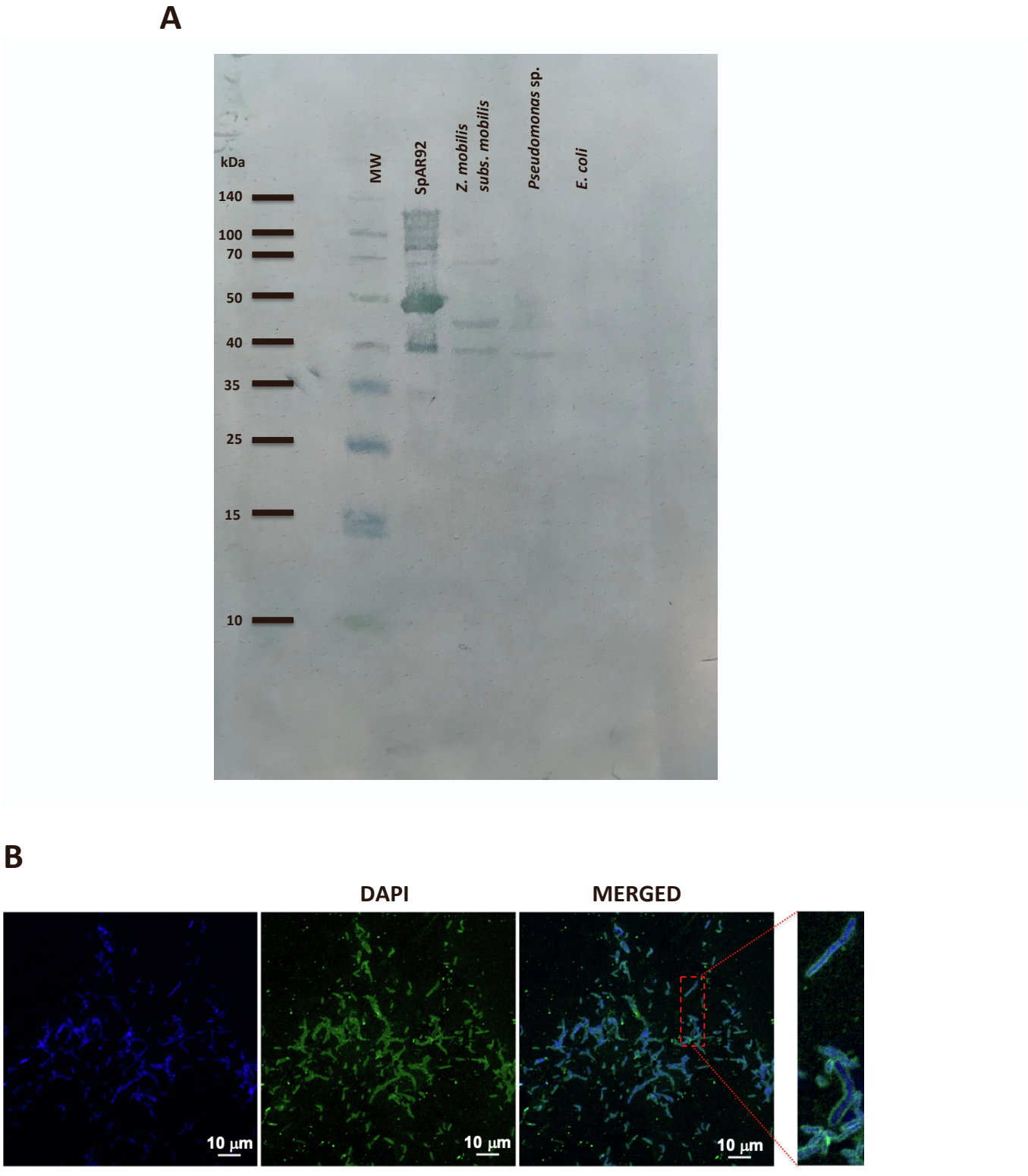

Figure S3. Specificity of anti-*Sphingomona* antibodies, Related to Figure 2C. (A) Total proteins were extracted from SpAR92, *Zymomonas mobilis* subsp. *mobilis* NRRL B-806, *Pseudomonas* sp. and *Escherichia coli* 086. Ten µg of total proteins from each bacterium were loaded onto a 12% SDS-polyacrylamide pre-cast gel and used for Western blot analysis using purified rabbit IgGs against SpAR92 membrane proteins. The membrane was incubated with an anti-rabbit IgG-HRP conjugate and finally developed with TMB (3,3′, 5,5′- tetramethylbenzidine) stabilized substrate for HRP. MW, molecular weight markers. (B) Anti-*Sphingomonas* SpAR92

rabbit IgGs were used as primary antibodies diluted 1:100 in 3% BSA/PBS. SpAR92 cells were fixed and incubated with the primary antibodies for 14 h at 4 °C. After the incubation, cells were washed three times in PBS and then incubated for 1 h with the secondary anti-rabbit IgG FITC conjugated antibody (Sigma-Aldrich) diluted 1:50 in 3% BSA/PBS. Cells were washed twice with PBS and mounted in ProLong Antifade reagent (Thermo Fisher Scientific). The sections were examined using a Zeiss LSM 800 laser scanning confocal microscope (Carl Zeiss, Oberkochen, Germany) with oil immersion objectives.

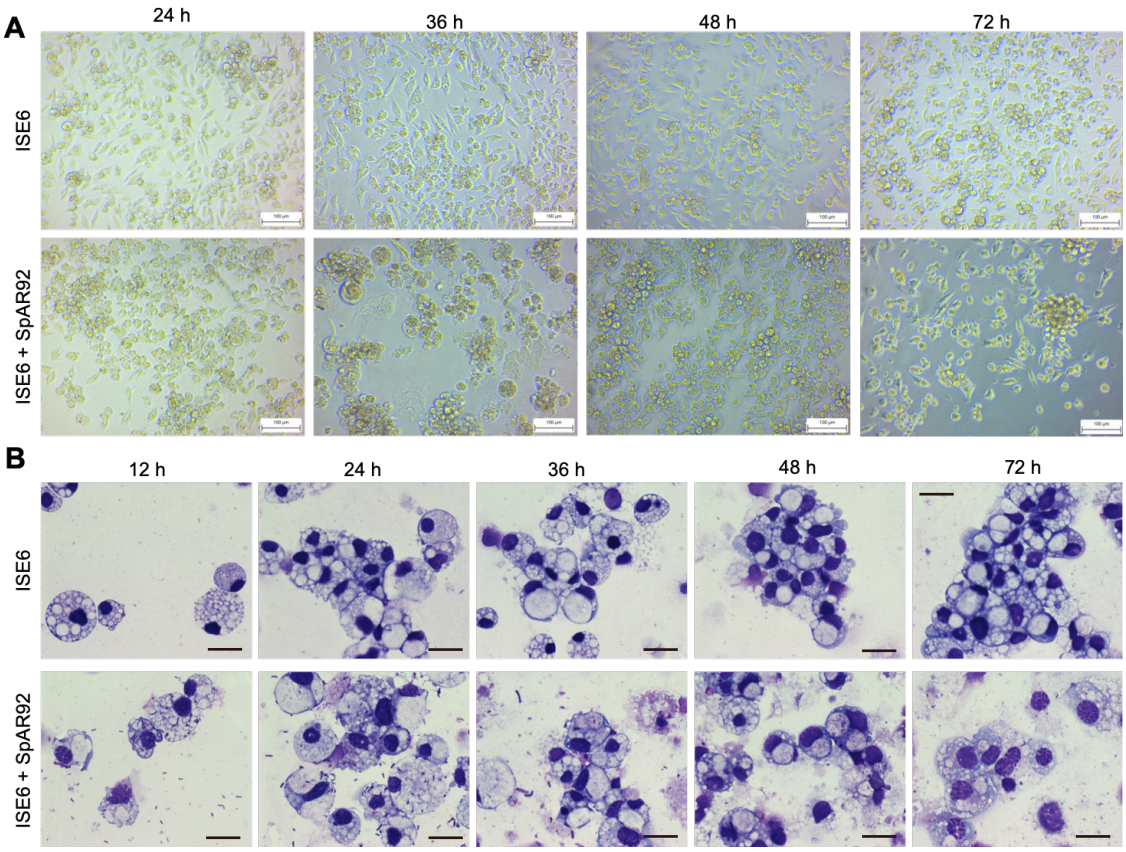

Figure S4. Effect of SpAR92 on uninfected ISE6 tick cells, Related to Figure 3C. An increase in apoptotic cells was observed in ISE6 cells cultured with SpAR92. Uninfected ISE6 cells were cultured in L-15B300:R2A (1:1) medium with and without SpAR92 and samples collected at different time points. (A) Phase contrast images. Bars, 100 µm. (B) Giemsa-stained cells. Bars, 10 µm.

A

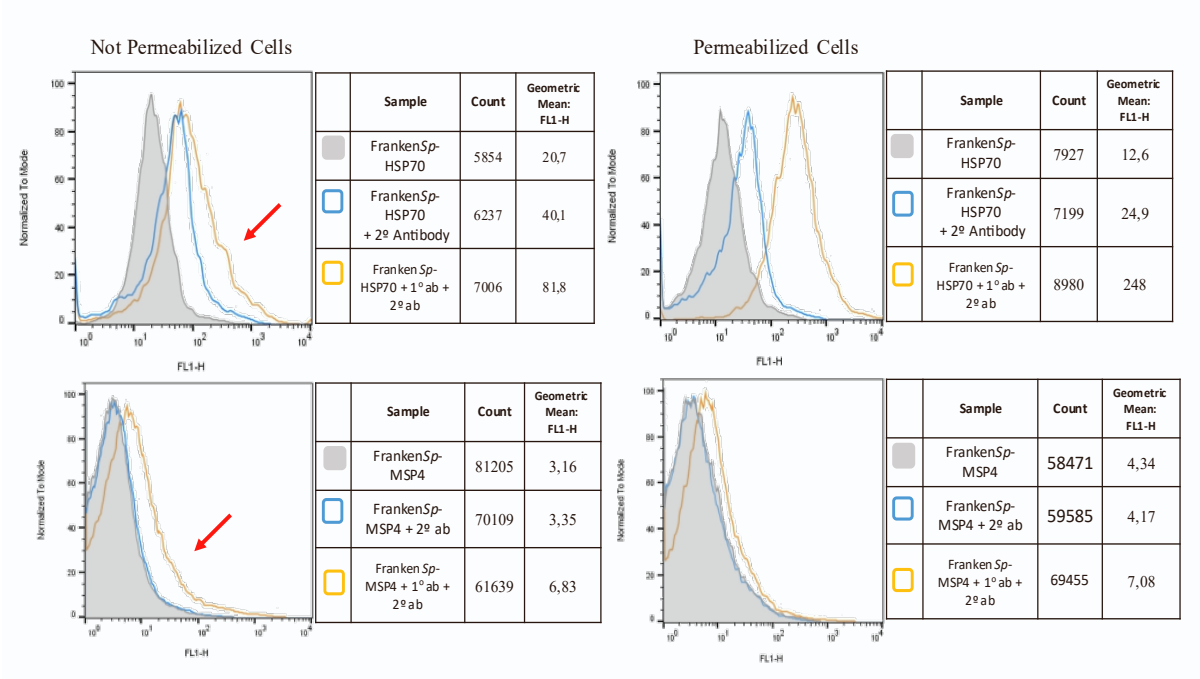

B

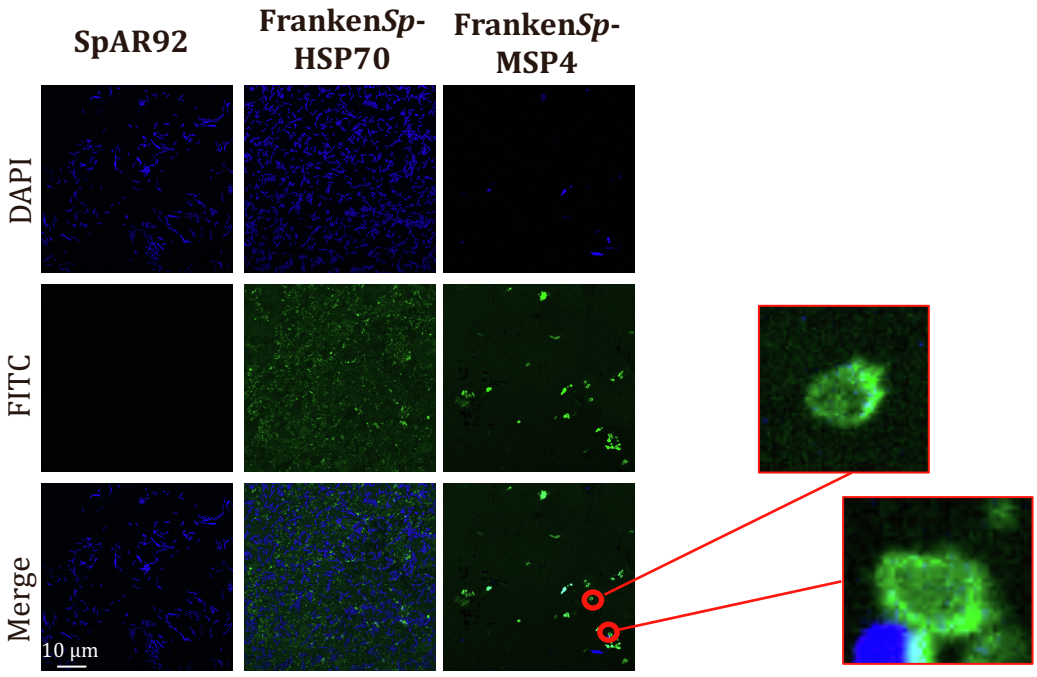

Figure S5. Validation of protein production on Franken*Sphingomonas* by flow cytometry and immunofluorescence, Related to Figures 5A and 5B. (A) Histograms and analysis for HSP70 and MSP4 protein production by flow cytometry on Franken*Sphingomonas* non-permeabilized (left) and permeabilized (right). Franken*Sp* (SpAR92 carrying pVHD-*hsp70* or pVHD-*msp4*) alone (grey) or with secondary antibody (blue) were used as negative controls. Confirmation of HSP70 and MSP4 on Franken*Sphingomonas* membrane surface is indicated with red arrows. (B) Representative images of immunofluorescence analysis of Franken*Sphingomonas*. Protein production was induced by the addition of 250 µM Vanillate. Cytospin preparation were incubated with MSP4 and HSP70 primary antibodies (green, FITC) and mounted on Prolong Diamon Antifade Mountant with DAPI reagent (blue). The localization of MSP4 protein on cell membrane is illustrated in Franken*Sphingomonas*-MSP4.